

g FACTOR, EFFECTIVE MASS, AND EXCHANGE SPLITTING IN PURE AND COBALT-DOPED Pd†

Sven Hörnfeldt*, J. B. Ketterson, and L. R. Windmiller

Argonne National Laboratory, Argonne, Illinois 60439

(Received 29 September 1969)

Measurements of the de Haas-van Alphen effect in pure and cobalt-doped palladium have been performed. Data on the effective mass and *g* factor are presented for pure Pd. Measurements on the ferromagnetic alloys clearly show the existence of an itinerant component in the magnetization.

The addition of a few tenths of a percent of cobalt or iron is sufficient to cause palladium to become ferromagnetic at low temperatures.^{1,2} It is of interest to know if an exchange splitting is observable in the palladium "bands." If the measured bulk magnetization is interpreted in terms of an effective local moment for the impurity atom, one obtains a value approaching 9 Bohr magnetons for very dilute alloys of cobalt in palladium,¹ and thus (since cobalt has a spin of two) one concludes that the palladium electrons in the vicinity of the impurity site are highly polarized. Neutron-diffraction measurements³ show that the radius of the polarization cloud is approximately equal to the average cobalt-cobalt spacing for a 0.1 at.% alloy. If the polarization clouds overlap we expect a spontaneous magnetization at zero field (for $T < T_c$). If the clouds do not overlap (i.e., a concentration much less than 0.1%), we expect an added magnetization in the presence of an external magnetic field due to the alignment of the clouds. We assume that the 9 Bohr magnetons associated with each cobalt impurity arise only partly from localized electrons, which contribute a moment not greatly different from the cobalt atomic moment of $2\mu_B$. We assume the remaining $7\mu_B$ arise from the magnetization of conduction-band electrons. Thus, we anticipate an exchange splitting of the Fermi surface in both of these cases.

The band structure⁴⁻⁶ and Fermi surface of pure palladium^{7,8} have been studied extensively. The agreement between theory and experiment is quite good and this aspect of the problem can be considered to be well understood.

Since the exchange splitting is expected to be small, one needs an experiment which is capable of high resolution in order to observe such a splitting. Very high resolution is available with the de Haas-van Alphen (dHvA) technique since the phase of the oscillations is quite high. The orbit diameters are much larger than the Co-Co spacing so that an average Fermi surface is sampled. The exchange splitting energy causes

an area shift $\Delta A = (dA/dE)\Delta E^{\text{ex}} = \pi m^* \Delta E^{\text{ex}}$ (where m^* is the cyclotron effective mass) for the extremal cross-sectional areas associated with the spin-up and spin-down sheets of a given surface. One would observe this area shift as a beat frequency in the de Haas-van Alphen signal. If the magnetization were completely local in character (i.e., no exchange splitting of the Pd bands) then no beats would be observed. To verify the existence of an exchange splitting one must observe at least one null and to evaluate the magnitude of the shift two nulls are required; i.e., $\Delta A = (2\pi e/\hbar c)H_1 H_2 / (H_1 - H_2)$, where H_1 and H_2 are the fields at which the two beat nulls occur.

Single crystals of palladium with 0.05 and 0.10 at.% Co and resistance ratios of 42 and 34, respectively, were used in the alloy portion of this experiment. The constituents were weighed on a precision balance and melted together in a water-cooled silver boat.⁹ The resulting rods were zone leveled and formed into single crystals (in an argon atmosphere) using an rf-heated floating zone refiner of special design.¹⁰ In these alloys we observed dHvA signals for both the ellipsoidal hole pocket (located at the point X of the Brillouin zone) and the Γ -centered electron surface. No signals from the open-hole surface were observed. Figures 1(a) and 1(b) show the dHvA oscillations associated with the ellipsoidal hole pocket for the 0.05 and 0.1% alloys, respectively. The magnetic field was along the [100] axis of the crystals, which corresponds to the lightest effective mass and thus the most easily observable period. For the 0.05% alloy, one beat null is clearly resolved and a second may also exist at lower fields where the signal is just emerging from the noise. We will assume the existence of this low-field beat null. For the 0.10% alloy, two beat nulls are clearly observable. The observation of the beat period in these alloys provides conclusive evidence for band magnetism.

The observed beats cannot be explained in terms of a beating with the other two symmetry-equivalent ellipsoids. [The weak fast beat in

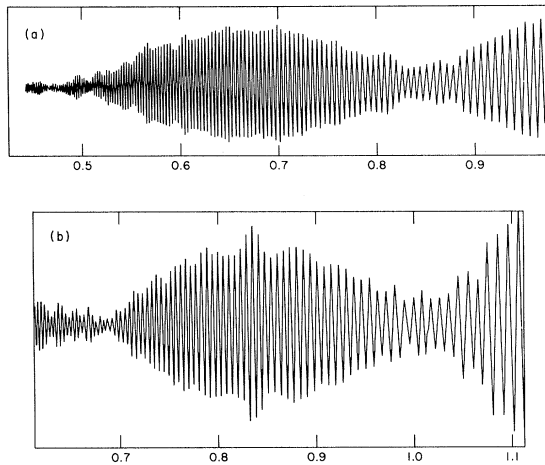


FIG. 1. The dHvA oscillations associated with the principal ellipsoid (centered at X) for the field along $[100]$ in (a) 0.05- and (b) 0.1-at.% Co-Pd alloys. The beats arise from an exchange splitting of the bands. The horizontal axis shows the magnetic field in volts. The calibration constant of the magnet is 49.82 kG/V.

Fig. 1(b), in fact, arises from these two ellipsoids.]

From the observed beat frequency we calculate the area shifts $\Delta A(0.05\%) = 1.40 \times 10^{-4}$ and $\Delta A(0.10\%) = 2.87 \times 10^{-4}$ a.u. The resulting energy shifts are $\Delta E(0.05\%) = 1.09 \times 10^{-4}$ and $\Delta E(0.10\%) = 2.23 \times 10^{-4}$ Ry, where we use the unenhanced band mass of 0.41.⁵ If this exchange splitting were constant over the surface and, moreover, the same for all sheets of the surface, the total band contribution to the saturation magnetization would be given by

$$m_s^{\text{band}} = \frac{1}{2} \mu_B N(E_F) \Delta E^{\text{ex}}.$$

Using the value⁵ $N(E_F) = 32$ states/atom Ry, this gives $m_s^{\text{band}}(0.05\%) = 1.09$ and $m_s^{\text{band}}(0.10\%) = 2.24$ emu/cm³. These values are much smaller than the values $m_s^{\text{band}}(0.05\%) = 2.2$ and $m_s^{\text{band}}(0.10\%) = 4.4$ emu/cm³ which correspond to a band magnetization of $7\mu_B$ per cobalt. We believe this discrepancy to arise primarily from an exchange splitting which is different for each sheet of the Fermi surface, largest for the heavy hole sheet, and which varies over each sheet. The value of μ_{eff} is extrapolated to be $9\mu_B$ for very dilute alloys of Co in Pd². However, any inaccuracy in the value $\mu_{\text{eff}} = 9\mu_B$ or in the assumed moment $\mu_{10c} = 2\mu_B$ of the electrons localized on each cobalt site must be much too small to account for the above discrepancy.

The Γ -centered electron surface was observed only over the limited magnetic-field range from

about 55 to 72 kG, this latter field being the limit of the magnetic field available with our superconducting solenoid. With this field range we were not able to resolve any beat waists. At several field angles we were, however, able to see a small reduction of the dHvA amplitude with increasing field. This indicates the onset of a beat null which would occur somewhere above our maximum available field. Using the field range over which we could observe the Γ -centered electron surface and an unenhanced effective cyclotron mass of 1.34,⁵ we can estimate that the exchange splittings for this surface must be substantially less than 1.5×10^{-4} and 1.8×10^{-4} Ry for the 0.05 and 0.1% alloys, respectively.

Thus, while the available field range is not large enough to allow any conclusion to be drawn about the exchange splitting of the Γ -centered electron surface in the 0.05% alloy, the exchange splitting on this surface is considerably less than on the X -centered pocket for the 0.1% alloy. This result supports our assumption that the exchange splitting ΔE^{ex} varies from sheet to sheet of the Fermi surface. It is not unreasonable that the splitting is small on the Γ -centered surface since this surface is largely s -like in character and since the exchange splitting arises primarily from the d -like part. The X -centered pocket on the other hand is almost entirely d -like.

In addition to observing beat nulls, there is an alternative method for verifying the existence of exchange splitting. This involves the effect of an exchange splitting on the "spin-splitting zeros" (in the dHvA amplitude) which are often observed in nonferromagnetic materials. In order to make our point clear we must explain this phenomenon. The individual Landau levels are separated by an energy $\hbar\omega_c = e\hbar H/m^*(\theta, \varphi)c$. In addition, the magnetic moment associated with a conduction electron causes each Landau level to be split into two levels separated by an energy $2\mu H = g(\theta, \varphi)e\hbar H/2m_0c$. Note that in crystals the g factor can deviate considerably from the free-space value of 2. If the g factor has a magnitude such that $gm^*/2m_0 = r + \frac{1}{2}$, then the spacing between two adjacent Landau levels is $\hbar\omega_c/2$. Under this circumstance the first harmonic of the dHvA amplitude disappears independently of field magnitude and we call this phenomenon a spin-splitting zero. If there is an exchange splitting, then the spin-splitting zero phenomenon no longer exists since the exchange splitting must be added to the spin splitting and this results in beating between the spin-up and spin-down dHvA periods.

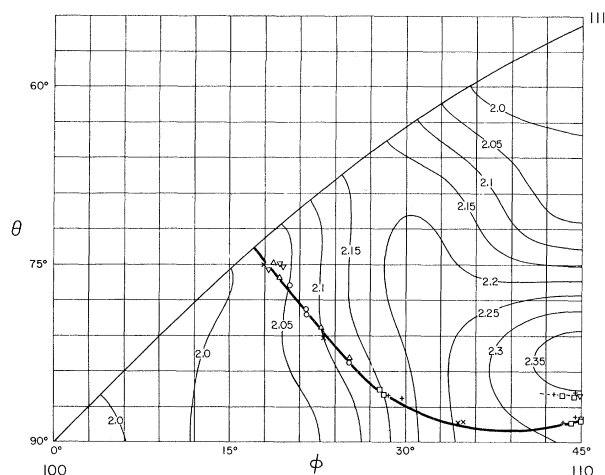


FIG. 2. The basic 1/48 of the unit sphere showing the polar coordinates of the observed spin-splitting zeros for the Γ -centered electron surface of Pd. Shown also are the contours of constant effective cyclotron mass which result from a fit to the masses observed in the dHvA experiments (Ref. 7). The different types of points (triangles, etc.) refer to the different planes in which dHvA data were observed.

The points in Fig. 2 show the angles at which the first harmonic of the dHvA amplitude was observed to disappear for the Γ -centered electron surface in pure Pd. The dark lines are contours connecting these points. These data are displayed in the basic 1/48th of the unit sphere and resulted from experimental runs in which the magnetic field was rotated in six different crystallographic planes. The solid contours drawn with light lines show the contours of constant effective mass $m^*(\theta, \varphi)$. These contours were generated by fitting cyclotron effective-mass data taken in four different crystallographic planes (using the temperature dependence of the dHvA amplitude) to a 27-term cubic harmonic expansion.⁷ If the g factor had its free-space value of 2.0, then the spin-splitting zero contour would coincide with a $2.5m_0$ effective-mass contour which does not occur in Pd. If the g factor were different from 2.0 but constant in magnitude, then the spin-splitting zero contour would run "parallel" to an effective-mass contour. Figure 2 clearly shows that the g factor in Pd is different from 2.0 and anisotropic. A similar situation exists in Pt.¹¹ Figure 3(a) shows the Γ -centered electron dHvA amplitude in the 0.05% alloy as the magnetic field is rotated in an arbitrary plane, a so-called field-rotation diagram. The oscillations result from the angular dependence of the dHvA area. The arrow indicates the mag-

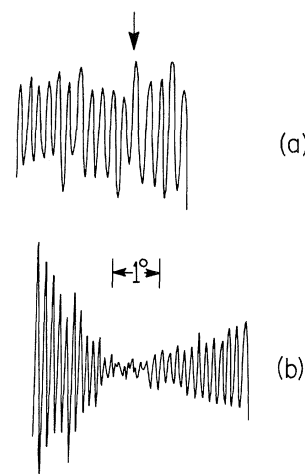


FIG. 3. (a) A field-rotation diagram in a 0.05-at.% Co-Pd alloy. The arrow indicates the angle at which the magnetic field direction intersects the spin-splitting zero contour. The intersection angle is $\theta = 80^\circ$, $\varphi = 23^\circ$, where θ and φ are measured from the appropriate $\langle 100 \rangle$ axis. (b) The almost identical field rotation in pure Pd (the field is however different). Note the clearly observable null in the amplitude.

netic field direction in which the dHvA amplitude disappears in pure Pd. Since the amplitude is quite large in the vicinity of this angle, we conclude that there is no spin-splitting zero, i.e., there is an exchange splitting. Figure 3(b) shows an almost identical field rotation in pure Pd. Note the clear observation of a spin-splitting zero (the field rotations were carried out at different fields and thus the different spacing between the oscillations).

Measurements of the temperature dependence of the magnetization were made on our 0.05% alloy¹² and it was determined that the Curie temperature was approximately 3 K. The magnetic fields available for this measurement were not sufficient to saturate the specimen and thus a value for μ_{eff} could not be determined.

The work discussed here will be expanded to include higher concentrations and larger magnetic fields. Concurrent measurements of the saturation magnetizations will also be included in order that the magnetization of the actual specimens under investigation may be determined.

In conclusion we would like to acknowledge stimulating discussions with K. Bennemann, J. Garland, and A. Ron.

†Based on work performed under the auspices of the U. S. Atomic Commission.

*Present address: Uppsala University, Uppsala, Sweden.

¹R. M. Bozorth, P. A. Wolff, D. D. Davis, V. B. Compton, and J. H. Wernick, *Phys. Rev.* **122**, 1157 (1961).

²J. Crangle and W. R. Scott, *J. Appl. Phys.* **36**, 921 (1965).

³G. G. Low and T. M. Holden, *Proc. Phys. Soc. (London)* **89**, 119 (1966).

⁴A. J. Freeman, J. O. Dimmock, and A. M. Furdyna, *J. Appl. Phys.* **37**, 1256 (1966).

⁵O. K. Anderson and A. R. Mackintosh, *Solid State Commun.* **6**, 285 (1968).

⁶F. M. Mueller, A. J. Freeman, J. O. Dimmock, and A. M. Furdyna, to be published.

⁷L. R. Windmiller, J. B. Ketterson, and S. Hornfeldt, *J. Appl. Phys.* **40**, 1291 (1969), and to be published.

⁸J. J. Vuillemin, *Phys. Rev.* **144**, 396 (1966).

⁹S. Hornfeldt, J. B. Ketterson, and L. R. Windmiller, *J. Cryst. Growth* **5**, 289 (1969).

¹⁰J. B. Ketterson, J. S. Tait, and L. R. Windmiller, *J. Cryst. Growth* **1**, 323 (1967).

¹¹L. R. Windmiller and J. B. Ketterson, *Phys. Rev. Letters* **21**, 1076 (1968).

¹²These measurements were kindly carried out by Dr. D. J. Lam of this laboratory.

MAGNETIC FORM FACTOR OF THULIUM METAL*

T. O. Brun

Ames Laboratory, Iowa State University, Ames, Iowa 50010

and

G. H. Lander

Ames Laboratory, Iowa State University, Ames, Iowa 50010, and

Argonne National Laboratory, Argonne, Illinois 60439

(Received 15 August 1969)

The magnetic form factor of thulium at 4.2°K has been measured with polarized neutrons. With the exception of the two innermost reflections, the form factor is in excellent agreement with the theoretical $4f^{12}$ form factor. At low angles an additional contribution to the form factor is present. We have interpreted this as $5d$ -like conduction-electron polarization, although the magnitude is unexpectedly large.

The crystal structure of thulium is hcp with $a = 3.537 \text{ \AA}$ and $c = 5.504 \text{ \AA}$. At 4.2°K the magnetic structure^{1,2} consists of ferromagnetic layers, in which the spins are aligned parallel (positive layers) or antiparallel (negative layers) to the c axis, stacked such that four positive layers are followed by three negative layers. The ordered moment per atom is $7\mu_B$, and the net ferromagnetic moment is $1\mu_B$ per atom. In the present experiment the magnetization density of this ferromagnetic component has been measured accurately with polarized neutrons. Recent magnetization measurements³ on a single crystal of thulium give the saturated moment per atom as $(1.001 \pm 0.005)\mu_B$ in low fields applied parallel to the c axis. For fields greater than 28 kOe, applied in the same direction, thulium becomes ferromagnetic, with a saturation moment of $(7.14 \pm 0.02)\mu_B$ per atom. The $0.14\mu_B$ in excess of $7\mu_B$ has been attributed to conduction-electron polarization.⁴ In the paramagnetic state (above 56°K) the effective moment is $7.61\mu_B$ per atom. The moments determined by neutron diffraction and magnetization experiments are consistent with the $4f^{12}$ configuration ($J=6$, $L=5$, $S=1$, $g=7/6$).

The form factor of terbium⁵ has been measured with both polarized and unpolarized neutrons. Reference 5 contains a detailed discussion of the form-factor derivation, and of the nature of the spin distribution in the rare earths. In comparison with terbium the present experiment with thulium has two immediate advantages. Firstly, the ferromagnetic scattering amplitude in the forward direction (p_0) is less than the nuclear scattering amplitude (b), which is not the case in terbium with a ferromagnetic moment of $9\mu_B$ per atom; this is important in considering the sensitivity of the polarized-beam method at low scattering angles. Secondly, the asphericity in the spin distribution for thulium is theoretically greater than for terbium, and may be readily observed.

The cross section for polarized neutron scattering has been given by Blume,⁶ and, considering the coherent elastic scattering only,

$$\begin{aligned}
 (d\sigma/d\Omega) \propto b^2 + 2\vec{P} \cdot \vec{\eta}_\perp b p_{\text{ferro}} + \eta_\perp^2 p_{\text{ferro}}^2 \\
 + \text{magnetic terms,} \quad (1)
 \end{aligned}$$

where \vec{P} is a vector in the direction of the neu-